bioRxiv preprint doi: https://doi.org/10.1101/2020.02.12.945469; this version posted February 12, 2020. The copyright holder for this preprint (which was not certified by peer review) is the author/funder, who has granted bioRxiv a license to display the preprint in perpetuity. It is made available under aCC-BY 4.0 International license.

The PINK1 – Parkin mitophagy signalling pathway is not functional in peripheral blood mononuclear cells

Aaron V. Bradshaw[1], Philip Campbell[1], Anthony H. V. Schapira[1], Huw R. Morris[1], Jan-Willem Taanman[1]*

[1]Department of Clinical and Movement Neurosciences, Queen Square Institute of Neurology, Royal Free Campus, University College London, London, United Kingdom

* Corresponding author

E-mail: j.taanman@ucl.ac.uk (JWT)

bioRxiv preprint doi: https://doi.org/10.1101/2020.02.12.945469; this version posted February 12, 2020. The copyright holder for this preprint (which was not certified by peer review) is the author/funder, who has granted bioRxiv a license to display the preprint in perpetuity. It is made available under aCC-BY 4.0 International license.

Abstract

Mutations in the *PINK1* and *PRKN* genes are the most common cause of early-onset familial Parkinson disease. These genes code for the PINK1 and Parkin proteins, respectively, which are involved in the degradation of dysfunctional mitochondria through mitophagy. An early step in PINK1 – Parkin mediated mitophagy is the ubiquitination of the mitofusin proteins MFN1 and -2. The ubiquitination of MFN1 and -2 in patient samples may therefore serve as a biomarker to determine the functional effects of *PINK1* and *PRKN* mutations, and to screen idiopathic patients for potential mitophagy defects. We aimed to characterise the expression of the PINK1 – Parkin mitophagy machinery in peripheral blood mononuclear cells (PBMCs) and assess if these cells could serve as a platform to evaluate mitophagy via analysis of MFN1 and -2 ubiquitination. Mitophagy was induced through mitochondrial depolarisation by treatment with the protonophore CCCP and ubiquitinated MFN proteins were analysed by western blotting. In addition, *PINK1* and *PRKN* mRNA and protein expression levels were characterised with reverse transcriptase quantitative PCR and western blotting, respectively. Whilst CCCP treatment led to MFN ubiquitination in primary fibroblasts, SH-SY5Y neuroblastoma cells and Jurkat leukaemic cells, treatment of PBMCs did not induce ubiquitination of MFN. *PRKN* mRNA and protein was readily detectable in PBMCs at comparable levels to those observed in Jurkat and fibroblast cells. In contrast, PINK1 protein was undetectable and *PINK1* mRNA levels remarkably low in control PBMCs. Our findings suggest that the PINK1 – Parkin mitophagy signalling pathway is not functional in PBMCs**.** Therefore, PBMCs are not a suitable biosample for analysis of mitophagy function in Parkinson disease patients.

bioRxiv preprint doi: https://doi.org/10.1101/2020.02.12.945469; this version posted February 12, 2020. The copyright holder for this preprint (which was not certified by peer review) is the author/funder, who has granted bioRxiv a license to display the preprint in perpetuity. It is made available under aCC-BY 4.0 International license.

Introduction

Parkinson disease (PD) has a heterogeneous clinical presentation. An important goal in PD research is to identify if and how this heterogeneity is related to biochemical and cell biological differences, which inform the pathophysiology of the disease [1]. The identification of such differences is important for three interrelated reasons: (1) the elucidation of mechanistic targets for drug development, (2) the selection of the most appropriate patient cohorts for clinical trials, and (3) to provide functional readouts allowing the identification of target engagement and changes in cellular and biochemical phenotypes.

Although most cases of PD are idiopathic, there are some rare early-onset familial forms, which may provide insights into potential biochemical subtypes that exist within the wider, idiopathic PD population. The most common forms of early-onset familial PD are caused mutations in the *PINK1* and *PRKN* genes, which encode PTEN induced putative kinase 1 (PINK1) [2] and Parkin, respectively [3]. Both proteins act in the same quality control pathway to sense damaged mitochondria and target them for degradation through a specialised form of marco-autophagy, also known as mitophagy. PINK1 is a mitochondrial kinase imported into the mitochondria via the preprotein translocase complexes where it is constitutively degraded by the presenilin-associated rhomboid-like protein (PARL) [4]. Loss of mitochondrial membrane potential disrupts the mitochondrial import and degradation of PINK1, which subsequently accumulates on the outer mitochondrial membrane (OMM) [5]. Here, PINK1 undergoes autophosphorylation [6] and phosphorylates Parkin at serine 65, promoting its mitochondrial translocation and stabilisation [7]. Phosphorylation of ubiquitin at serine 65 by PINK1 further promotes the full activation of Parkin [8, 9]. Parkin, an E3 ubiquitin ligase ubiquitinates multiple OMM proteins, including mitofusin 1 (MFN1) and mitofusin 2 (MFN2) [10]. Recruitment of autophagy adaptors by ubiquitin chains conjugated to OMM proteins [11] leads to the engulfment of impaired mitochondria by autophagosomes, which fuse with lysosomes causing the eventual degradation of defective mitochondria.

The clinical, molecular and functional genetics of *PINK1* and *PRKN* are complex. Disease causing mutations can include missense mutations, deletions and copy number variations, which can be inherited in homozygous and compound heterozygous patterns [2, 3, 12, 13]. Pathogenic *PINK1* and *PRKN* mutations are generally associated with a loss of function of the respective proteins. Furthermore, recent findings demonstrate that heterozygously inherited *PINK1* mutations can confer increased PD risk, an effect that may be mediated at the molecular level by a dominant negative mechanism during PINK1 dimerisation [14, 15]. However, the effects of these mutations on Parkin and PINK1 function, and on downstream mitophagy, have not been fully characterised. For instance, there are over 200 *PRKN* variants, some of which are pathological and which have differing effects

bioRxiv preprint doi: https://doi.org/10.1101/2020.02.12.945469; this version posted February 12, 2020. The copyright holder for this preprint (which was not certified by peer review) is the author/funder, who has granted bioRxiv a license to display the preprint in perpetuity. It is made available under aCC-BY 4.0 International license.

on Parkin function and mitophagy [16]. Moreover, mitophagy is impaired in skin fibroblasts from PD patients with no known genetic cause [17, 18]. These findings suggest that defects in mitophagy may contribute to idiopathic PD in some patients [19].

Although the role of mitophagy in the pathogenesis of PD is debated, functional readouts of the PINK1 – Parkin mitophagy signalling pathway may provide patient stratification, even if they are epiphenomenal to disease causing processes. Such readouts will also allow the functional characterisation of novel *PINK1* and *PRKN* variants and those of unknown significance. One such functional readout is the ubiquitination of the MFN proteins following mitochondrial depolarisation, a lack of which distinguishes *PINK1* and *PRKN* mutant fibroblasts from those isolated from healthy controls [20]. In this study we aimed to translate this readout to peripheral blood mononuclear cells (PBMCs), which represent a minimally invasive source of biological tissue for biomarker analysis. We have also characterised the expression of the PINK1 – Parkin signalling pathway in different cell types and demonstrate that the pathway is not functional in PBMCs. This work thus adds an important contribution to knowledge on the mitochondrial biology of PBMCs and their utility in PD research.

Results

Treatment of fibroblasts with CCCP induces MFN ubiquitination in a PINK/Parkin dependent manner

We began by characterising the effect of mitochondrial depolarisation upon the ubiquitination of the OMM proteins MFN1 and MFN2 in primary fibroblast cultures. Fibroblasts from 2 healthy controls were treated with 20 µM carbonyl cyanide *m*-chlorophenyl hydrazone (CCCP) for 2 hours to depolarise the mitochondria followed by western blot analysis. In untreated cells, MFN1 was detected as a double band, with the lower and upper bands migrating at 75 and 78 kDa, respectively, and MFN2 was detected as a single band with an apparent M_r of 75 kDa (Fig 1). CCCP treatment led to the appearance of an extra anti-MFN1 reactive band, which migrated with an apparent M_r that was 9 kDa larger than the lower MFN1 band detected in untreated cells. In addition, an extra anti-MFN1 reactive band that was 9 kDa larger than the MFN2 band in untreated cells was detected (Fig 1). This size change is consistent with mono-ubiquitination and our previous work [10] indicates that the extra MFN1 and MFN2 bands detected post-CCCP treatment are ubiquitin positive. Next, we performed the same treatment and analysis on fibroblast cultures from two early-onset PD patients, one with a homozygous nonsense mutation in *PINK1* and one with a homozygous deletion in *PRKN*. Consistent with previous reports [20], CCCP treatment failed to

bioRxiv preprint doi: https://doi.org/10.1101/2020.02.12.945469; this version posted February 12, 2020. The copyright holder for this preprint (which was not certified by peer review) is the author/funder, who has granted bioRxiv a license to display the preprint in perpetuity. It is made available under aCC-BY 4.0 International license.

induce ubiquitination of either MFN1 or MFN2 in fibroblasts from either patient (Fig 1). These results demonstrate that CCCP-induced ubiquitination of MFN1 and MFN2 in fibroblasts depends upon the presence of functional PINK1 and Parkin proteins.

Treatment of Jurkat cells with CCCP induces MFN ubiquitination

We next asked whether CCCP-induced MFN ubiquitination was a shared feature across different cell types. We first opted to analyse the immortalised T-lymphocyte cell line Jurkat as a surrogate model for primary leucocyte cells. Similar to that observed in control fibroblasts, CCCP treatment produced extra anti-MFN1 and anti-MFN2-2 reactive bands, whose migration was consistent with mono-ubiquitination of the respective proteins (Fig 2A). In addition, we observed faint anti-MFN1 and anti-MFN2-2 reactive bands suggestive for polyubiquitination. Time course analysis demonstrated that CCCP-induced ubiquitination of MFN1 and MFN2 occurred as early as 30 minutes post-treatment and persisted up to 24 hours post-treatment (Fig 2B). The maximum ubiquitinated MFN signal was detected at 2 hours post-treatment, for both MFN1 and MFN2 (S1 Fig). Thus, Jurkat cells respond in the same way as fibroblasts to CCCP treatment in terms of MFN ubiquitination.

Treatment of PBMCs from healthy controls with CCCP does not induce MFN ubiquitination

Following these findings, we aimed to compare the CCCP-induced MFN ubiquitination response across 4 different cell types: the immortalised neuroblastoma SH-SY5Y cell line, the immortalised Jurkat T-lymphocyte cell line, primary cultured fibroblasts and PBMCs derived from healthy controls. Similarly to the results obtained with fibroblasts and Jurkat cells, and consistent with our previous report [10], treatment of SH-SY5Y cells with CCCP produced an anti-MFN1 and anti-MFN2 reactive profile consistent with ubiquitination (Fig 3). As demonstrated in Figs 1 and 2, anti-MFN1 and anti-MFN2 reactive bands consistent with mono-ubiquitination were also detected in CCCP-treated Jurkat cells and fibroblasts; however, we did not detect anti-MFN1 and anti-MFN2 reactive bands consistent with MFN ubiquitination in CCCP-treated PBMC samples (Fig 3). Long exposure images also did not reveal any signal consistent with ubiquitination of either MFN1 or -2. These results demonstrate that under the conditions tested, CCCP treatment does not induce ubiquitination of MFN1 or -2 in PBMCs.

Parkin is expressed in PBMCs from healthy controls

bioRxiv preprint doi: https://doi.org/10.1101/2020.02.12.945469; this version posted February 12, 2020. The copyright holder for this preprint (which was not certified by peer review) is the author/funder, who has granted bioRxiv a license to display the preprint in perpetuity. It is made available under aCC-BY 4.0 International license.

In order to shed light on lack of CCCP-induced MFN ubiquitination in PBMCs, we next determined the relative expression of PINK1 and Parkin. We began by assessing the relative abundance of *PRKN* transcripts in Jurkat, fibroblast, SH-SY5Y and PBMC samples. RNA was isolated from the cells and reverse transcribed to create cDNA libraries from which *PRKN* transcripts were amplified by real-time quantitative PCR (qPCR). *PRKN* mRNA was readily amplified from all cell types, and when normalised, fibroblasts (2 independent cultures) and SH-SY5Y cells exhibited 11.8, 10.2 and 12.6 times the *PRKN* levels detected in Jurkat cells (Fig 4A). *PRKN* transcripts were also amplified from 5 independent control PBMC cultures. Levels in these cultures were similar to those detected in Jurkat cells (Fig 4A).

By western blot analysis, Parkin protein was readily detected in 3 independent control fibroblast cultures as well as in Jurkat cells and SH-SY5Y cells as a single band migrating at ~48 kDa (Fig 4B). SH-SY5Y cells demonstrated the highest Parkin signal (~23 fold more than Jurkat and fibroblast cells, Fig 4D). A ~48-kDa band was also detected in PBMC samples from 6 healthy controls (Fig 4C). This protein co-migrated with that detected in SH-SY5Y cells and Jurkat cells, and importantly, was absent from HeLa cells, which have been demonstrated to not express Parkin protein [21]. Therefore, we assume that the ~48-kDa band detected in PBMCs represents Parkin. Quantitatively, the Parkin signal from PBMCs was not significantly different from that detected in either Jurkat or fibroblast cells (Fig 4D). Collectively, these findings demonstrate that Parkin is expressed in PBMCs and, consequently, that the lack of CCCP-induced MFN ubiquitination in these cells is not due to a lack of Parkin expression.

PINK1 is undetectable in PBMCs from healthy controls

In order to investigate the expression levels of *PINK1* mRNA in PBMCs, RNA was isolated from Jurkat, fibroblast, SH-SY5Y and PBMC samples and followed by reverse transcriptase qPCR. *PINK1* transcript levels in fibroblasts exceeded those detected in Jurkat cells by 33.8 and 32.7 times (for two independent control cultures), whilst levels in SH-SY5Y cells were similar to those in Jurkat cells (Fig 5A). Levels of *PINK1* mRNA in PBMCs from healthy controls were 20–100 times lower than those detected in Jurkat cells and >3000 times lower than those detected in fibroblast cultures (Fig 5A).

PINK1 protein is constitutively degraded by PARL in the mitochondria and, as a result, undetectable under basal conditions. In order to detect PINK1, the mitochondrial membrane potential must be dissipated, for example with prolonged CCCP treatment. Therefore, control fibroblasts, SH-SY5Y cells, Jurkat cells and PBMCs were treated with 20 µM CCCP for 24 hours, followed by western blot analysis for PINK1. PINK1 antibodies have been reported to give a panoply

bioRxiv preprint doi: https://doi.org/10.1101/2020.02.12.945469; this version posted February 12, 2020. The copyright holder for this preprint (which was not certified by peer review) is the author/funder, who has granted bioRxiv a license to display the preprint in perpetuity. It is made available under aCC-BY 4.0 International license.

of non-specific bands when used in western blotting, including at the predicted M_r of PINK1, as determined in knockout cells [22]. Such observations may confound the interpretation of results and render the use of biological controls as critical when studying PINK1 protein. Indeed, even in untreated cells we detected numerous cross reactive bands in fibroblast, SH-SY5Y and Jurkat samples with a PINK1 antibody from Novus Biologicals (Fig 5B). However, when these cells were treated with CCCP, an additional band appeared at ~60 kDa, the predicted molecular weight of mature PINK1 (Fig 5B). This band was absent in untreated cells and is, thus, consistent with PINK1. The levels of PINK1 protein were significantly higher in Jurkat cells than either fibroblast or SH-SY5Y cells. Fibroblast cells expressed the lowest levels of PINK1 after CCCP treatment, 10 times lower than detected in Jurkat cells (Fig 5C). However, in PBMCs the pattern of PINK1 cross reactive proteins was unchanged between treated and untreated cells (Fig 5B). Specifically we did not detect an additional band at 60 kDa when cells were treated with CCCP, thus suggesting that PINK1 protein is not detectable in PBMCs. With an alternative PINK1 antibody from Cell Signaling Technologies, we also failed to detect PINK1 in CCCP-treated PBMCs, despite adequate detection in the other cell types (S2 Fig). The lack of PINK1 detection in PBMCs may explain the absence of CCCP-induced MFN ubiquitination in these cells.

During mitophagy, mitochondrial proteins are degraded in the lysosome. Accordingly, mitophagy can be monitored by assessing the levels of mitochondrial proteins post mitophagic induction. Indeed, in Jurkat, fibroblast and SH-SY5Y cells, 24 hour CCCP treatment led to significant reductions in subunit A of the mitochondrial succinate dehydrogenase complex (SDHA) (Fig 5D). In PBMCs, conversely, treatment with CCCP did not significantly affect SDHA levels (Fig 5D). These findings suggest differences in CCCP-induced mitophagy between cultured SH-SY5Y, fibroblast and Jurkat cells on the one hand, and PBMCs on the other.

The PINK1– Parkin mitophagy signalling pathway is not expressed in activated T cells and lymphoblastoid cell lines

PBMCs cultured under normal conditions are non-proliferative, whereas Jurkat cells are robustly proliferating T lymphocyte-like cells. For that reason, we investigated whether inducing the proliferation of T cells in the PBMC samples would shift their response to CCCP treatment. Moreover, we analysed how Epstein-Barr virus (EBV) immortalised lymphoblastoid cell lines (LCLs) from healthy controls responded to CCCP treatment. The T-cell fraction of PBMCs were induced to proliferate by incubation with T-activator CD3/CD28 Dynabeads. This treatment led to the appearance of cell clusters, which were visually similar to cell clusters observed in both Jurkat and LCL cultures (Fig 6A). Despite these morphological similarities, neither activated PBMCs nor LCLs

bioRxiv preprint doi: https://doi.org/10.1101/2020.02.12.945469; this version posted February 12, 2020. The copyright holder for this preprint (which was not certified by peer review) is the author/funder, who has granted bioRxiv a license to display the preprint in perpetuity. It is made available under aCC-BY 4.0 International license.

responded to 2-hour CCCP treatment with ubiquitination of MFN1 or MFN2 (Fig 6B). Furthermore, PINK1 protein did not accumulate in either cell type following prolonged CCCP treatment (Fig 6C). *PINK1* mRNA levels in LCLs were also 10–25 times lower than those detected in fibroblasts (S3 Fig). As shown in Fig 4, western blot analysis detected Parkin in Jurkat cells and non-proliferating PBMCs; however, Parkin was undetectable in PBMCs activated with CD23/CD8 Dynabeads and in 4 independent LCLs (Fig 6D). Collectively, these findings demonstrate that whilst Jurkat cells exhibit CCCP-induced PINK1 – Parkin signalling, this pathway is absent from activated PBMCs and LCLs.

Discussion

In this study we aimed to assess the utility of PBMCs as a platform for studying mitophagy defects in PD patients. Our analysis demonstrated that PBMCs are unsuitable for this purpose as they do not functionally express the PINK1 – Parkin mitophagy signalling pathway. The ubiquitination of MFN proteins following CCCP treatment can be used as a marker of early mitophagy in fibroblasts, and distinguishes control fibroblasts from those with *PINK1* or *PRKN* mutations [20]. Our findings demonstrate that this process is not conserved in all cell types. Specifically, PBMCs and lymphocytes immortalised by EBV transduction lack the necessary machinery to transduce loss of mitochondrial membrane potential into MFN ubiquitination.

In agreement with previous work, we detected *PRKN* mRNA and Parkin protein in PBMCs from healthy controls [23, 24]. Parkin is a multi-functional protein with roles in diverse cellular processes, including those related to immunity [25]. Its expression in these cells is thus expected. However, we were unable to detect PINK1 protein in PBMCs, and levels of *PINK1* mRNA in these cells were remarkably low, up to 3000 times lower than those detected in fibroblast cells. The low levels of PINK1 expression in PBMCs likely explains their lack of CCCP-induced MFN ubiquitination, as PINK1 accumulation is required to activate Parkin on the mitochondrial surface [8]. PINK1 protein was also undetectable in LCLs and mRNA levels were 10–25 times lower than those detected in fibroblasts.

Jurkat cells underwent CCCP-induced MFN ubiquitination and time dependent reduction in SDHA levels, indicating functional mitophagy similar to that observed in fibroblasts and SH-SY5Y cells. Moreover, Jurkat cells expressed readily detectable levels of *PINK1* and *PRKN* mRNA and the respective proteins. Jurkat cells are an EBV-negative T-cell line derived from an acute lymphoblastic leukaemia biopsy, and proliferate rapidly in culture [26, 27]. We thus considered that it may have been the quiescence of primary PBMCs, which rendered them insensitive to CCCP-induced mitophagy. However, stimulation of PBMCs with CD3/CD28 antibodies, whilst leading to robust proliferation [28], did not result in CCCP-induced MFN ubiquitination. In fact, stimulated PBMCs

bioRxiv preprint doi: https://doi.org/10.1101/2020.02.12.945469; this version posted February 12, 2020. The copyright holder for this preprint (which was not certified by peer review) is the author/funder, who has granted bioRxiv a license to display the preprint in perpetuity. It is made available under aCC-BY 4.0 International license.

massively downregulated Parkin expression. PBMCs isolated from patients are a heterogeneous cellular sample [29], and this reduction in Parkin expression post-stimulation may have been due to the clonal expansion of PBMC sub-populations lacking Parkin expression. In favour of this hypothesis, we noted that EBV-transformed lymphocytes from four independent controls did not express Parkin protein at detectable levels. It is tempting to speculate that the lack of Parkin in these immunoactive cells may reflect a specific function. For instance, the downregulation of Parkin in blood cells may promote viral clearance through promoting mitochondrial ROS production [30].

Conclusions

Overall, our findings demonstrate PBMCs from control subjects do not undergo MFN ubiquitination after acute induction of mitophagy with CCCP. PBMCs express extraordinarily low *PINK1* mRNA levels and PINK1 protein is undetectable. The physiology of these cells thus precludes their use as a platform in studying the PINK1 – Parkin mitophagy signalling pathway in PD research.

Methods

Attainment of samples

Primary human dermal fibroblast cultures were established from skin explants of two early-onset PD patients, one female patient with a homozygous p.R246X nonsense mutation in *PINK1* and a heterozygous deletion of exons 4–6 in *PRKN*, and one female patient with a homozygous deletion of exons 4–5 in *PRKN*. In addition, skin biopsies were obtained from age-matched healthy control subjects. Fibroblast cultures were established according to standard procedures [31]. Ethical approval for this work was obtained from the Royal Free Hospital and Medical School Research Ethics Committee (REC 07/H0720/161). Ethical approval for PBMC work was obtained from Camden and King's Cross Research Ethics Committee (REC 17/LO/1166). All donors provided prior informed written consent and all work was performed in compliance with national legislation and the Declaration of Helsinki.

PBMC isolation, culture and treatment

PBMCs were isolated using standard Ficoll gradient separation protocols. Blood collected in EDTA-coated vacutainer blood tubes was mixed with an equal volume of phosphate-buffered saline (PBS). Diluted blood (20 ml) was layered on to 15 ml of Lymphoprep (Stemcell Technologies) in 50-ml Falcon tubes and centrifuged at 400× *g* for 30 min without deceleration. The resultant PBMC layer was then aspirated into a new 15-ml Falcon tube and washed twice in PBS, centrifuging at 300× *g* to

bioRxiv preprint doi: https://doi.org/10.1101/2020.02.12.945469; this version posted February 12, 2020. The copyright holder for this preprint (which was not certified by peer review) is the author/funder, who has granted bioRxiv a license to display the preprint in perpetuity. It is made available under aCC-BY 4.0 International license.

reduce platelet contamination. Fresh PBMCs were then re-suspended in RPMI medium (Thermo Fisher Scientific, 61870) and counted using a flow cytometer (Moxi GO™, Orflo Technologies).

For routine analysis, PBMCs were cultured at 1x10^6 cells/ml in RPMI supplemented with 10% foetal bovine serum (FBS) and 1 mM sodium pyruvate at 37°C, 5% CO_2. After 24 h, cells were treated with 20 μM CCCP and harvested at the indicated time points. For harvesting, 2 volumes of PBS were directly added to the suspended cells, followed by centrifugation at 500× *g* for 10 min. The pellet was resuspended in 1 ml of PBS and centrifuged at 17,000× *g* for 10 min at 4°C. The supernatant was aspirated and the pellet was stored at -80°C until further analysis. The age and sex of the donors of the PBMC samples used in this study are shown in S4 Table.

Culturing of fibroblasts, SH-SY5Y, Jurkat and LCLs

Primary human skin fibroblast cultures were grown in DMEM (Thermo Fisher Scientific, 61965-059) supplemented with 10% FBS, 1 mM sodium pyruvate, and 50 units/ml of penicillin and 50 μg/ml of streptomycin at 37°C, 5% CO_2. SH-SY5Y cells were cultured in DMEM: F12 (1:1) (Thermo Fisher Scientific, 31331-028) supplemented with 10% FBS, 1× non-essential amino acids and penicillin/streptomycin at 37°C, 5% CO_2. When confluent, cultures were passaged using trypsinisation. Jurkat cells and LCLs were cultured in suspension in RPMI medium 1640 (Thermo Fisher Scientific, 61870-127) supplemented with 10% FBS and 1 mM sodium pyruvate at 37°C, 5% CO_2. Cells were maintained at 5×10^5–3×10^6 cells/ml.

PBMC activation with CD3/CD28 Dynabeads

PBMCs were incubated with Dynabeads Human T-Activator CD3/CD28 (Thermo Fisher Scientific, 11132D) at a ratio of 1 : 1 and cultured in OpTmizer T-cell expansion SFM medium supplemented with 10 mM L-glutamine, penicillin/streptomycin, serum substitute (Thermo Fisher Scientific, A1048501) and 30 U/ml of interleukin-2 (IL-2; Thermo Fisher Scientific, PHC0026) at 37°C, 5% CO_2. Cultures were maintained at 1×10^6–3×10^6 cells/ml. Cells were activated for 7 days prior to analysis.

Reverse-transcriptase real-time quantitative PCR

RNA was isolated from cell pellets with the RNeasy kit (Qiagen, 74104) and quantified with a Nanodrop spectrophotometer (Thermo Fisher Scientific). RNA (500 ng) was reverse transcribed to produce cDNA libraries using the QuantiTect Reverse Transcriptase Kit from Qiagen (205311). cDNA was quantified by Qubit analysis with the 1× dsDNA HS Assay Kit (Thermo Fisher Scientific, Q33230).

bioRxiv preprint doi: https://doi.org/10.1101/2020.02.12.945469; this version posted February 12, 2020. The copyright holder for this preprint (which was not certified by peer review) is the author/funder, who has granted bioRxiv a license to display the preprint in perpetuity. It is made available under aCC-BY 4.0 International license.

For qPCR, 1 ng of cDNA was mixed with forward and reverse primers (final concentration 10 µM), PowerUp SYBR Green Master Mix (Thermo Fisher Scientific, A25780) and water to a final volume of 20 µl. Primers were purchased from Qiagen (*PRKN*: QT00023401; *PINK1*: QT00056630).

Following initial denaturation at 50°C for 2 min and activation at 95°C for 2 min, thermocycling was performed with 50 cycles of denaturation (94°C, 15 sec), annealing (55°C, 30 sec) and extension (72°C, 30 sec), using an Applied Biosystems StepOne real-time PCR system. Samples were analysed as technical triplicates. Fluorescence was read during the extension step. Melting temperature analysis was performed on the amplified products to ensure consistency within and between runs. Amplicon specific C_t thresholds were applied consistently between runs, and relative transcript levels were calculated by transforming the C_t values using the expression 2^{-Ct}, followed by normalisation to cDNA quantity.

Cell lysis and western blotting

Cell pellets were lysed in 0.1% Triton X-100 in PBS containing a Halt Protease Inhibitor Cocktail (Thermo Fisher Scientific; 78430). Lysates were vortexed and incubated for 15 min on ice, followed by clarification at 17,000× *g* for ten min at 4°C. Following determination of the protein concentration in the supernatants (Pierce™ BCA Protein Assay Kit; Thermo Fisher Scientific, 23250), samples were prepared for denaturing gel electrophoresis by addition of Laemmli Sample Buffer (BioRad, 161-0747), Sample Reducing Agent (Thermo Fisher Scientific, NP0009) and water to consistent protein concentrations.

Samples were resolved on Mini-Protean® TGX 4–20% gels or TGX 7.5% gels (BioRad Laboratories, 4568095 and 4568025). Separated proteins were transferred to Trans-Blot Turbo 0.2-µm PVDF membranes (BioRad, 170-4157), using the BioRad Trans-Blot Turbo Transfer System. Membranes were blocked in 10% non-fat dry milk powder in PBS prior to incubation with primary antibodies overnight at 4°C in 5% milk, 0.15% Tween-20, PBS. Following washing with 0.15% Tween-20, PBS, membranes were incubated with secondary antibodies conjugated to HRP enzymes (Dako, P0447 and P0448) and washed again. Blots were developed with Clarity Western ECL Substrate (BioRad, 170-5060). Capturing of the chemiluminescent signals was performed with the BioRad Chemidoc™ MP Imaging System. Signals were quantified with BioRad Image Lab 6.0.1 software. The primary antibodies are specified in S5 Table.

Statistical analyses

bioRxiv preprint doi: https://doi.org/10.1101/2020.02.12.945469; this version posted February 12, 2020. The copyright holder for this preprint (which was not certified by peer review) is the author/funder, who has granted bioRxiv a license to display the preprint in perpetuity. It is made available under aCC-BY 4.0 International license.

Graphs and statistical analyses were executed with GraphPad Prism® version 6.01 software. Data are presented as mean ± standard error of the mean. Student's t test was used to examine statistical significance and significance levels were set to $p<0.05$.

Acknowledgements

We would like to thank the Research Assistants John Harvey and Miriam Pollard for their work on the wider project of which this study was a part.

References

[1] Espay AJ, Brundin P, Lang AE. Precision medicine for disease modification in Parkinson disease. Nat Rev Neurol. 2017;13:119-126.

[2] Valente EM, Abou-Sleiman PM, Caputo V, Muqit MMK, Harvey K, Gispert S, et al. Hereditary early-onset Parkinson's disease caused by mutations in pink1. Science. 2004;304:1158-70.

[3] Kitada T, Asakawa S, Hattori N, Matsumine H, Yamamura Y, Minoshima S, et al. Mutations in the parkin gene cause autosomal recessive juvenile parkinsonism. Nature. 1998;392:605-8.

[4] Yamano K, Youle RJ. PINK1 is degraded through the n-end rule pathway. Autophagy. 2013;9:1758-69.

[5] Narendra DP, Jin SM, Tanaka A, Suen D, Gautier CA, Shen J, et al. PINK1 is selectively stabilized on impaired mitochondria to activate parkin. PLoS Biol. 2010;8:e1000298.

[6] Okatsu K, Oka T, Iguchi M, Imamura K, Kosako H, Tani N, et al. PINK1 autophosphorylation upon membrane potential dissipation is essential for parkin recruitment to damaged mitochondria. Nat Commun. 2012;3:1016.

[7] Kondapalli C, Kazlauskaite A, Zhang N, Woodroof HI, Campbell DG, Gourlay R, et al. PINK1 is activated by mitochondrial membrane potential depolarization and stimulates parkin E3 ligase activity by phosphorylating serine 65. Open Biol. 2012;2:120080.

[8] Kane LA, Lazarou M, Fogel AI, Li Y, Yamano K, Sarraf SA, et al. PINK1 phosphorylates ubiquitin to activate parkin E3 ubiquitin ligase activity. J Cell Biol. 2014;205:143-53.

[9] Koyano F, Okatsu K, Kosako H, Tamura, Go YE, Kimura M, Kimura Y, et al. Ubiquitin is phosphorylated by PINK1 to activate parkin. Nature. 2014;510:162-6

[10] Gegg ME, Cooper JM, Chau KY, Rojo M, Schapira AHV, Taanman J-W. Mitofusin 1 and mitofusin 2 are ubiquitinated in a PINK1/parkin-dependent manner upon induction of mitophagy. Hum Mol Genet. 2010;19:4861-70.

bioRxiv preprint doi: https://doi.org/10.1101/2020.02.12.945469; this version posted February 12, 2020. The copyright holder for this preprint (which was not certified by peer review) is the author/funder, who has granted bioRxiv a license to display the preprint in perpetuity. It is made available under aCC-BY 4.0 International license.

[11] Nguyen TN, Padman BS, Lazarou M. Deciphering the molecular signals of PINK1/Parkin mitophagy. Trends Cell Biol. 2016;26:733-744.

[12] Hattori N, Mizuno Y. Twenty years since the discovery of the parkin gene. J Neural Transm (Vienna). 2017;124:1037-1054.

[13] Huttenlocher J, Stefansson H, Steinberg S, Helgadottir HT, Sveinbjörnsdóttir S, Riess O, et al. Heterozygote carriers for CNVs in PARK2 are at increased risk of Parkinson's disease. Hum Mol Genet. 2015;24:5637-43.

[14] Puschmann A, Fiesel FC, Caulfield TR, Hudec R, Ando M, Truban D, et al. Heterozygous PINK1 p.G411S increases risk of Parkinson's disease via a dominant-negative mechanism. Brain. 2016;140:98-117.

[15] Gandhi S, Plun-Favreau H. Mutations and mechanism: how PINK1 may contribute to risk of sporadic Parkinson's disease. Brain. 2017;140:2-5.

[16] Yi W, Macdougall EJ, Tang MY, Krahn AI, Gan-Or Z, Trempe J, et al. The landscape of Parkin variants reveals pathogenic mechanisms and therapeutic targets in Parkinson's disease. Hum Mol Genet. 2019;28:2811-2825.

[17] Hsieh CH, Shaltouki A, Gonzalez AE, Da Cruz AB, Burbulla LF, St. Lawrence E, et al. Functional impairment in Miro degradation and mitophagy is a shared feature in familial and sporadic Parkinson's disease. Cell Stem Cell. 2016;19:709-724.

[18] Wang X. Destructive cellular paths underlying familial and sporadic Parkinson disease converge on mitophagy. Autophagy. 2017;13:1998-1999.

[19] Ryan BJ, Hoek S, Fon EA, Wade-Martins R. Mitochondrial dysfunction and mitophagy in Parkinson's: from familial to sporadic disease. Trends Biochem Sci. 2015;40:200-10.

[20] Rakovic A, Grünewald A, Kottwitz J, Brüggemann N, Pramstaller PP, Lohmann K, et al. Mutations in PINK1 and Parkin impair ubiquitination of mitofusins in human fibroblasts. PLoS ONE. 2011;6, e16746.

[21] Villa E, Proïcs E, Rubio-Patiño C, Obba S, Zunino B, Bossowski JP, et al. Parkin-independent mitophagy controls chemotherapeutic response in cancer cells. Cell Rep. 2017;20:2846-2859.

[22] Walsh TG, Van Den Bosch MTJ, Lewis KE, Williams CM, Poole AW. Loss of the mitochondrial kinase PINK1 does not alter platelet function. Sci Rep. 2018;8:14377.

[23] Sunada Y, Saito F, Matsumura K, Shimizu T. Differential expression of the parkin gene in the human brain and peripheral leukocytes. Neurosci Lett. 1998;254:180-2.

[24] Kasap M, Akpinar G, Sazci A, Idrisoglu HA, Vahaboğlu H. Evidence for the presence of full-length PARK2 mRNA and Parkin protein in human blood. Neurosci Lett. 2009;460:196-200.

bioRxiv preprint doi: https://doi.org/10.1101/2020.02.12.945469; this version posted February 12, 2020. The copyright holder for this preprint (which was not certified by peer review) is the author/funder, who has granted bioRxiv a license to display the preprint in perpetuity. It is made available under aCC-BY 4.0 International license.

399 [25] Manzanillo PS, Ayres JS, Watson RO, Collins AC, Souza G, Rae CS, et al. The ubiquitin ligase
400 parkin mediates resistance to intracellular pathogens. Nature. 2013;501:512-6.
401 [26] Schneider U, Schwenk HU, Bornkamm G. Characterization of EBV-genome negative 'null' and 'T'
402 cell lines derived from children with acute lymphoblastic leukemia and leukemic transformed
403 non-Hodgkin lymphoma. Int J Cancer. 1977;19:621-6.
404 [27] Gioia L, Siddique A, Head SR, Salomon DR, Su AI. A genome-wide survey of mutations in the
405 Jurkat cell line. BMC Genomics. 2018;19:334.
406 [28] Trickett A, Kwan YL. T cell stimulation and expansion using anti-CD3/CD28 beads. J Immunol
407 Methods. 2003;275:251-5.
408 [29] Grievink H, Tarik WL, Kluft C, Moerland M, Malone KE. Comparison of three isolation techniques
409 for human peripheral blood mononuclear cells: cell recovery and viability, population
410 composition, and cell functionality. Biopreserv Biobank. 2016;14:410-415.
411 [30] Li J, Ma C, Long F, Yang D, Liu X, Hu Y, et al. Parkin impairs antiviral immunity by suppressing the
412 mitochondrial reactive oxygen species-Nlrp3 axis and antiviral inflammation. iScience.
413 2019;16:468-484.
414 [31] Park IH, Lerou PH, Zhao R, Huo H, Daley GQ. Generation of human-induced pluripotent stem
415 cells. Nat Protoc. 2008;3:1180-6.

bioRxiv preprint doi: https://doi.org/10.1101/2020.02.12.945469; this version posted February 12, 2020. The copyright holder for this preprint (which was not certified by peer review) is the author/funder, who has granted bioRxiv a license to display the preprint in perpetuity. It is made available under aCC-BY 4.0 International license.

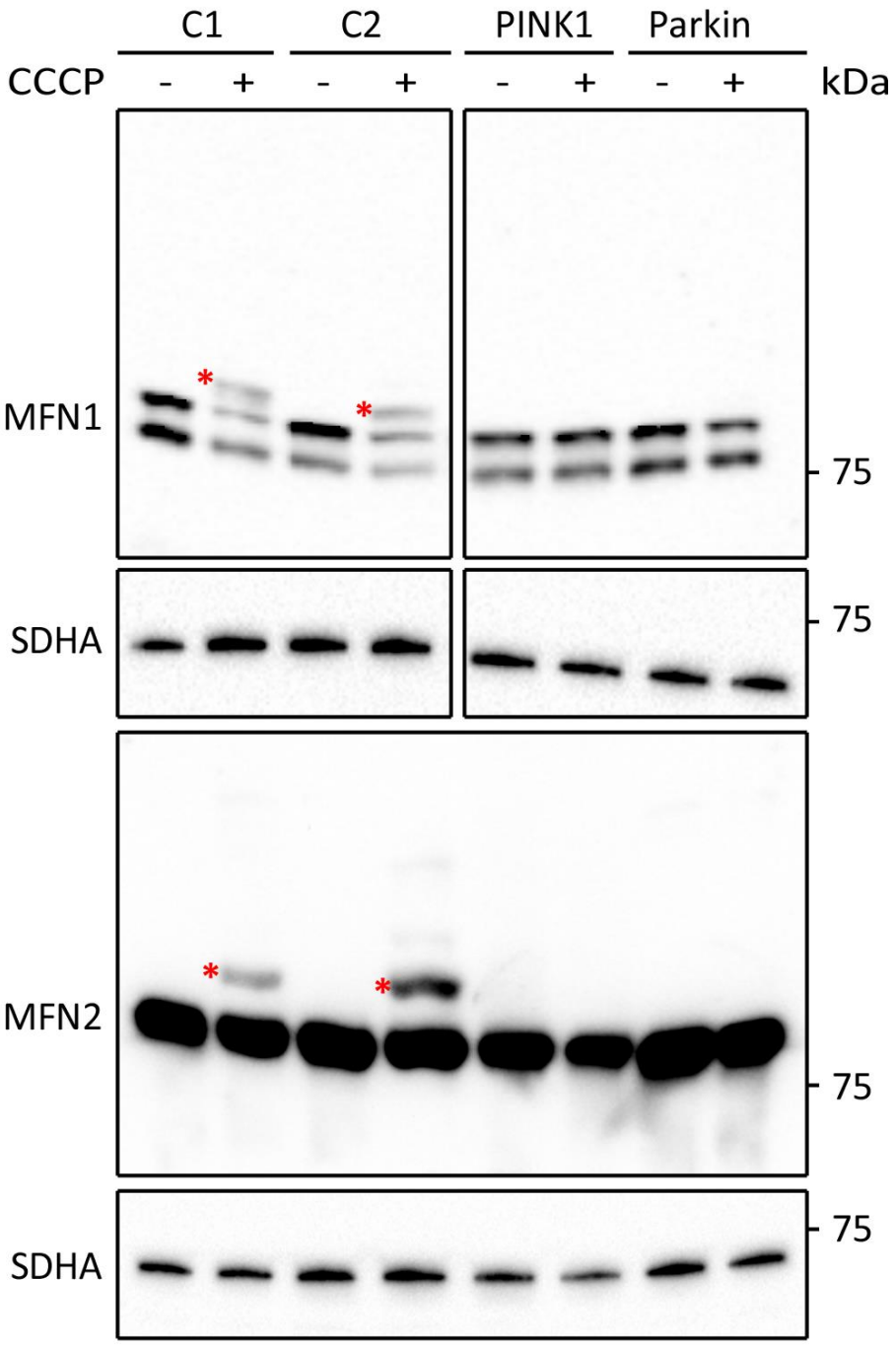

Fig 1. Analysis of CCCP-induced MFN ubiquitination in cultured fibroblast cells. Western blot analysis of fibroblasts from healthy controls (C1 and C2) and two early-onset PD patients with mutations in *PINK1* or *PRKN*. Cells were left untreated or were treated for 2 hours with 20 µM CCCP. Blots were developed with antibodies against MFN1 and MFN2. Antibodies against SDHA were used as loading control. Asterisks indicate bands representing ubiquitinated MFN proteins.

bioRxiv preprint doi: https://doi.org/10.1101/2020.02.12.945469; this version posted February 12, 2020. The copyright holder for this preprint (which was not certified by peer review) is the author/funder, who has granted bioRxiv a license to display the preprint in perpetuity. It is made available under aCC-BY 4.0 International license.

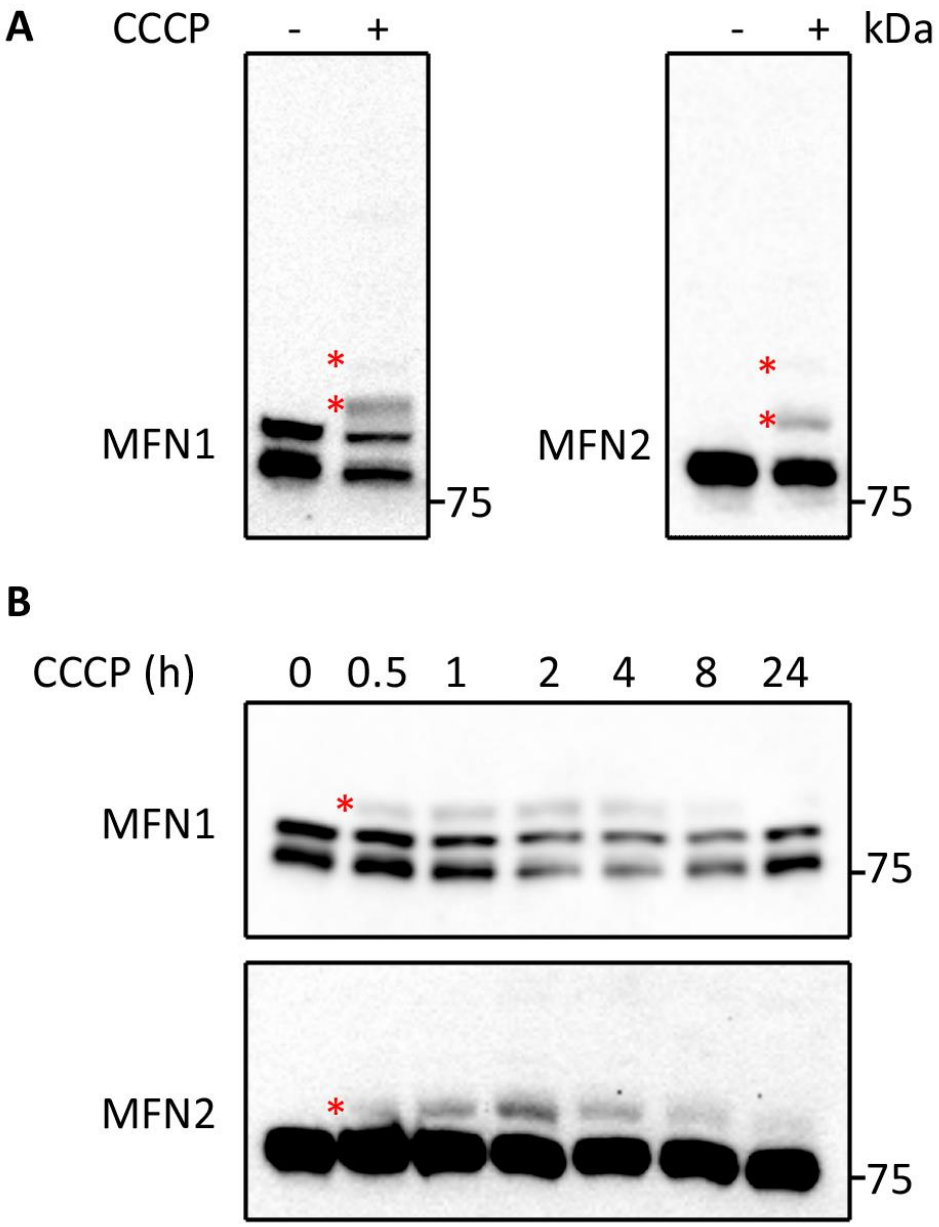

Fig 2. Analysis of CCCP-induced MFN ubiquitination in Jurkat cells. (A) Jurkat cells left untreated or treated for 2 hours with 20 μM CCCP were analysed by western blotting with antibodies against MFN1 and MFN2. (B) Western blot analysis of Jurkat cells treated with CCCP for increasing periods of time (0.5–24 hours), developed with antibodies against MFN1 and MFN2. Asterisks indicate bands representing ubiquitinated MFN proteins.

bioRxiv preprint doi: https://doi.org/10.1101/2020.02.12.945469; this version posted February 12, 2020. The copyright holder for this preprint (which was not certified by peer review) is the author/funder, who has granted bioRxiv a license to display the preprint in perpetuity. It is made available under aCC-BY 4.0 International license.

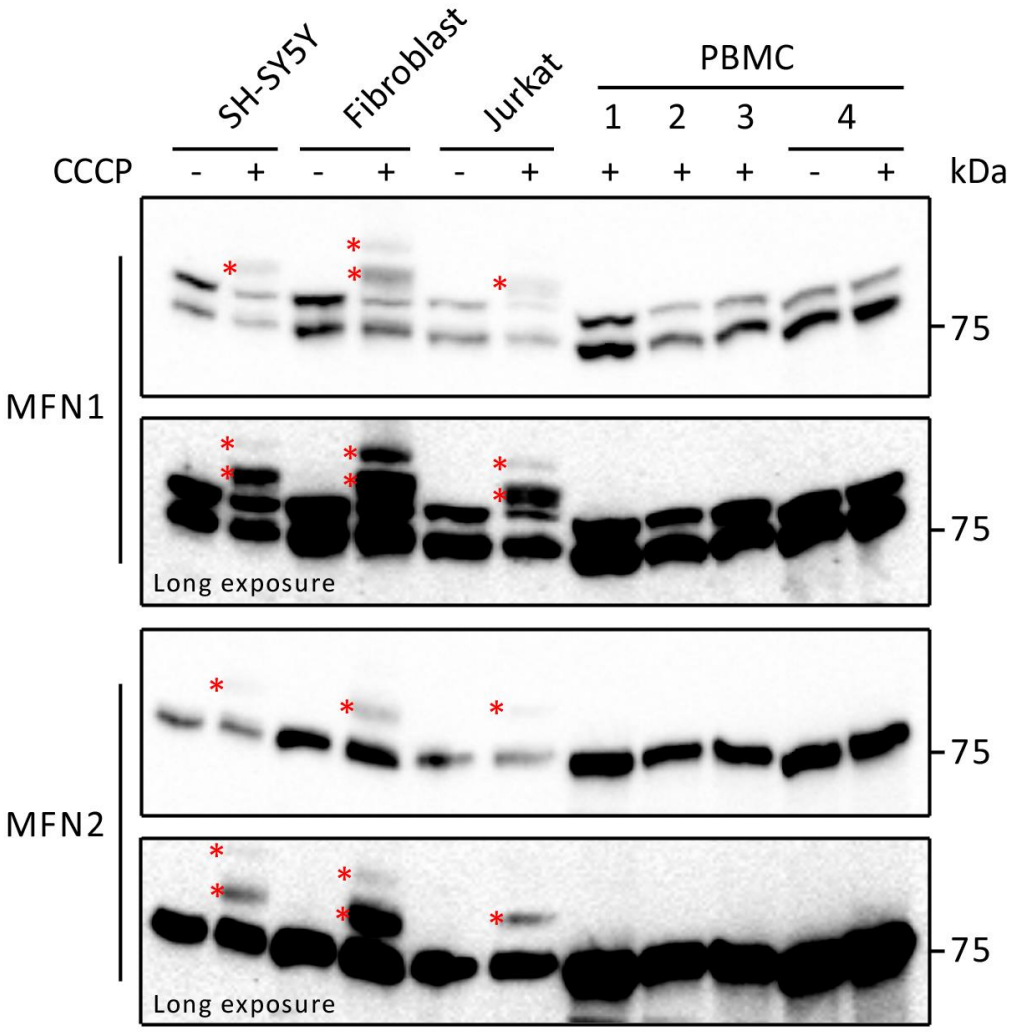

Fig 3. Analysis of CCCP-induced MFN ubiquitination in different cells types. SH-SY5Y, fibroblast, Jurkat and PBMC samples were left untreated or were treated with 20 µM CCCP for 2 hours and analysed by western blotting with antibodies against MFN1 and MFN2. Asterisks indicate bands representing ubiquitinated MFN proteins.

bioRxiv preprint doi: https://doi.org/10.1101/2020.02.12.945469; this version posted February 12, 2020. The copyright holder for this preprint (which was not certified by peer review) is the author/funder, who has granted bioRxiv a license to display the preprint in perpetuity. It is made available under aCC-BY 4.0 International license.

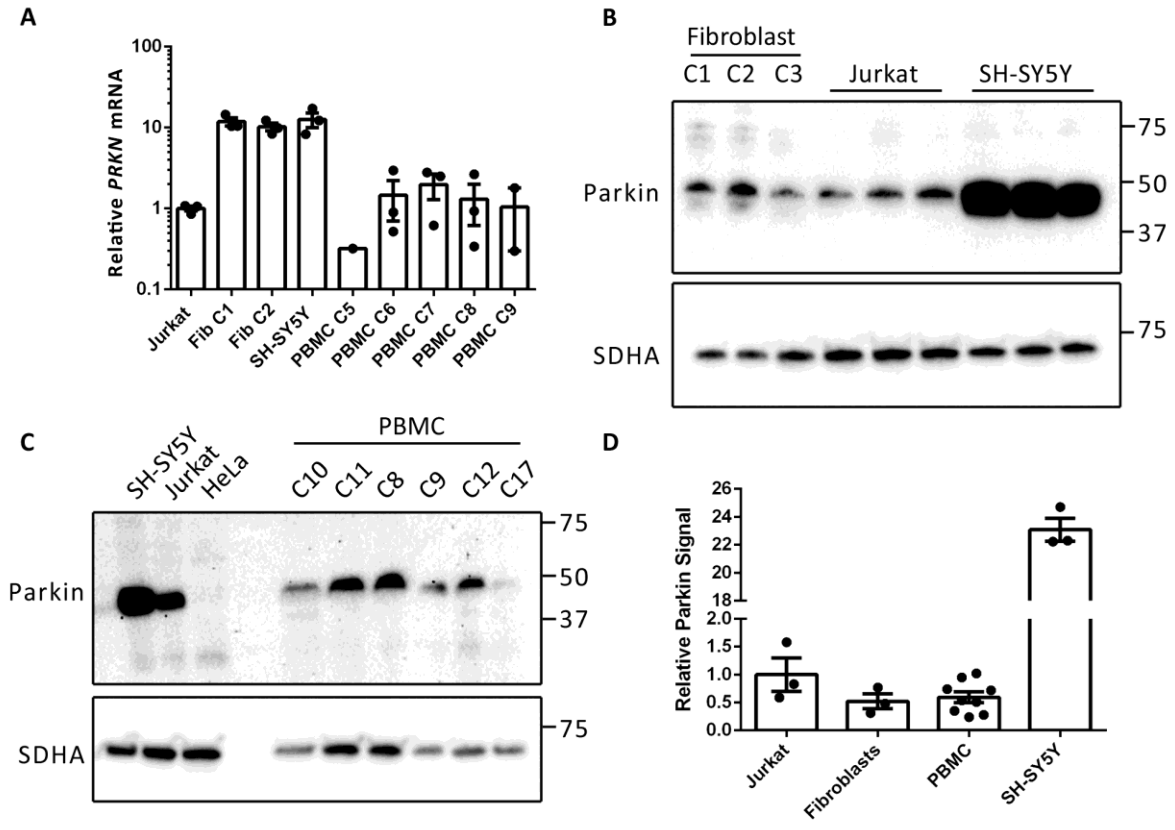

Fig 4. Analysis of Parkin expression in different cell types. (A) Reverse transcriptase qPCR analysis of *PRKN* mRNA levels in Jurkat, control fibroblast (Fib), SH-SY5Y and PBMC samples. qPCR was performed on equal amounts of cDNA from each cell type and C_t values were expressed relative to the Jurkat sample. (B, C) Western blot analysis of fibroblast, SH-SY5Y, Jurkat and PBMC cultures with an antibody against Parkin. (D) Quantification of Parkin signal in the different cell types. Signal is expressed relative to SDHA and normalised to that detected in Jurkat cells. Graphs display mean ± SEM.

bioRxiv preprint doi: https://doi.org/10.1101/2020.02.12.945469; this version posted February 12, 2020. The copyright holder for this preprint (which was not certified by peer review) is the author/funder, who has granted bioRxiv a license to display the preprint in perpetuity. It is made available under aCC-BY 4.0 International license.

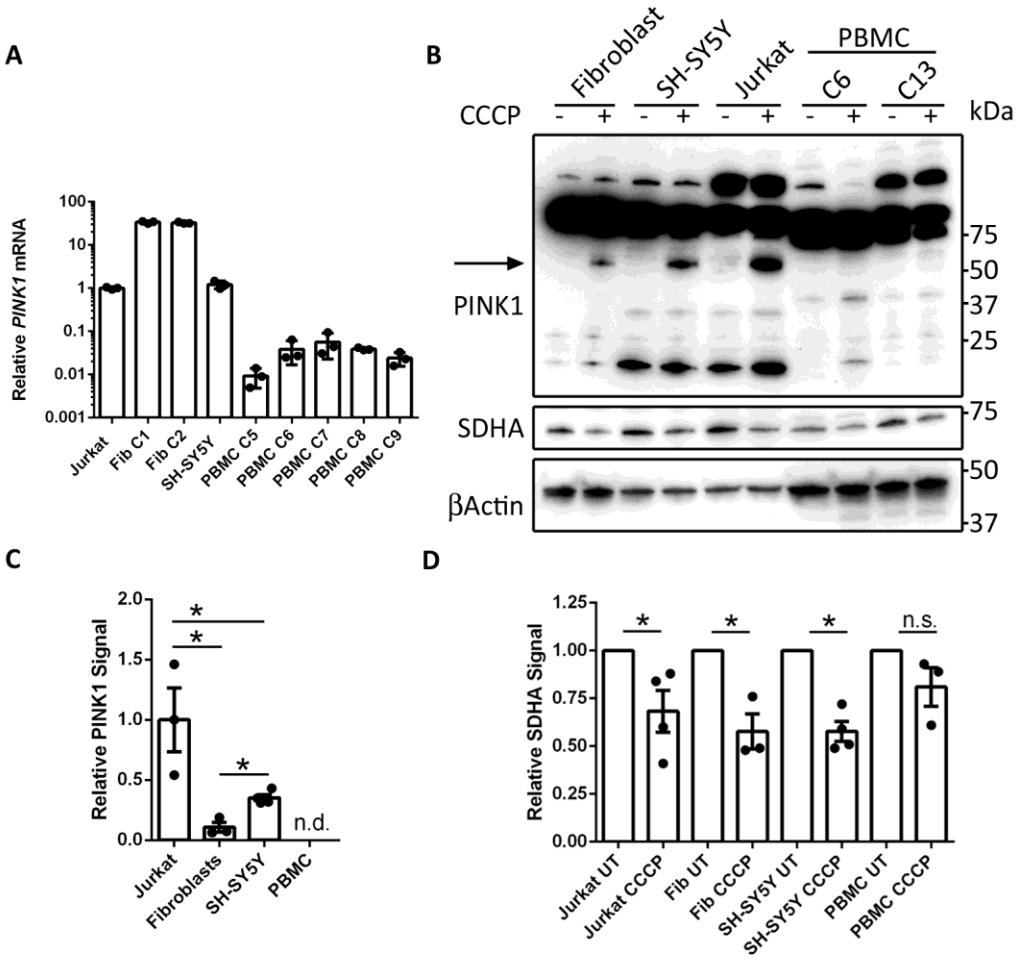

Fig 5. Analysis of PINK1 expression in different cell types. (A) Reverse transcriptase qPCR analysis of *PINK1* mRNA levels in Jurkat, control fibroblast (Fib), SH-SY5Y and PBMC samples. qPCR was performed on equal amounts of cDNA from each cell type and C_t values were expressed relative to the Jurkat sample. (B) Western blot analysis of fibroblasts, SH-SY5Y, Jurkat and PBMC cultures left untreated and treated with 20 µM CCCP for 24 hour with an antibody against PINK1 (Novus Biologicals, BC100-494). The band corresponding to PINK1 is indicated by the arrow. (C) Quantification of PINK1 signal from CCCP-treated cells. Signal is expressed relative to β-actin and normalised to levels detected in Jurkat cells. (D) Quantification of SDHA signal from untreated and 24-hour CCCP-treated Jurkat, fibroblast, SH-SY5Y and PBMC samples. Signal is expressed relative to β-actin and normalised to the untreated condition. Graphs display mean ± SEM; *=P<0.05, Student's t-test; n.d. = not detected; n.s. = not significant.

bioRxiv preprint doi: https://doi.org/10.1101/2020.02.12.945469; this version posted February 12, 2020. The copyright holder for this preprint (which was not certified by peer review) is the author/funder, who has granted bioRxiv a license to display the preprint in perpetuity. It is made available under aCC-BY 4.0 International license.

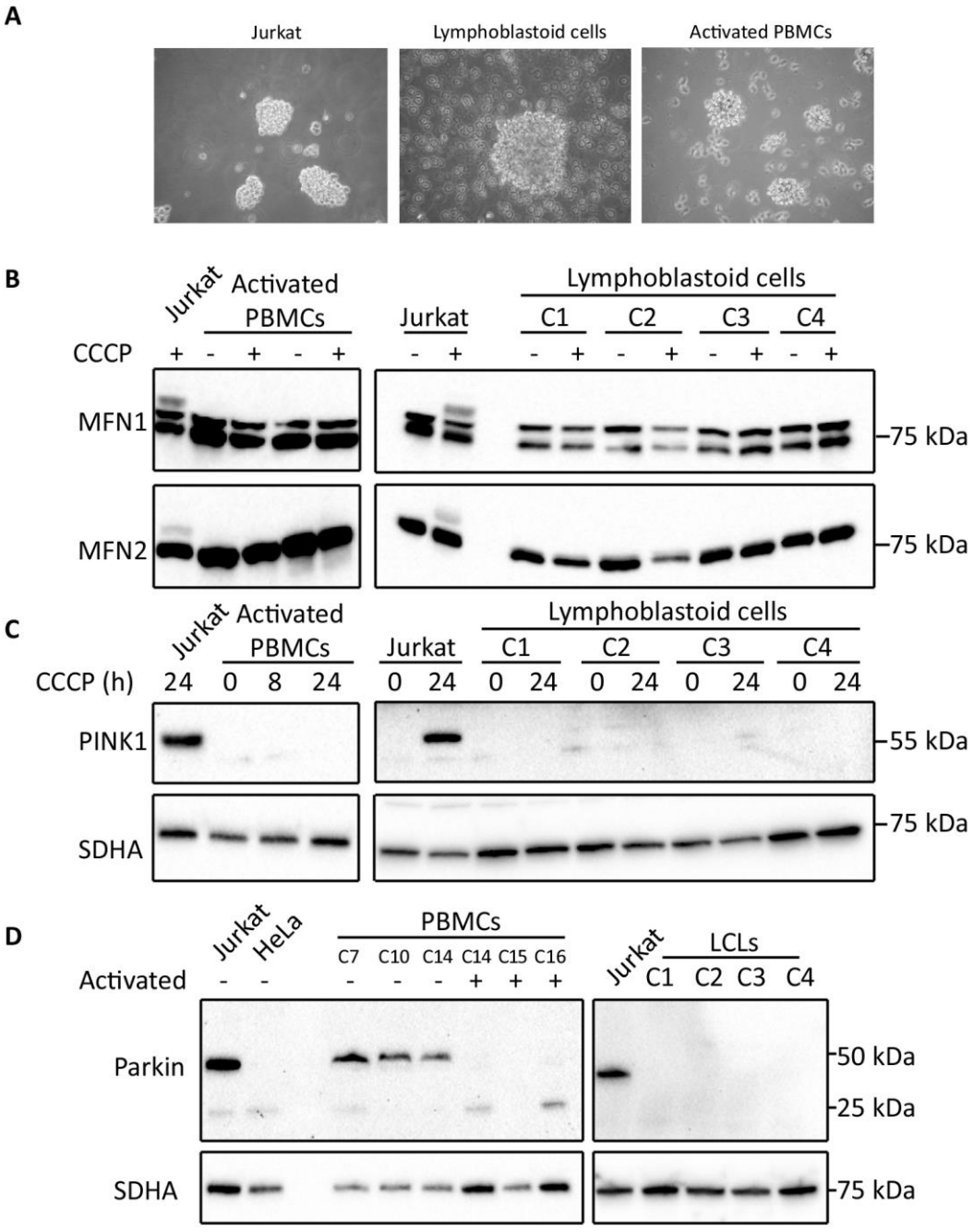

Fig 6. Analysis of PINK1 – Parkin signalling pathway in lymphoblastoid cell lines and CD3/CD28 activated PBMCs. (A) Phase contrast microscopy images of Jurkat cells, lymphoblastoid cell lines (LCLs) and CD3/CD28 Dynabead activated PBMCs. (B) Western blot analysis of MFN1 and -2 ubiquitination following CCCP treatment of activated PBMCs and LCLs. (C) Western blot analysis of PINK1 expression in activated PBMCs and LCLs following prolonged CCCP treatment. (D) Western blot analysis of Parkin expression in resting and CD3/CD28 Dynabead activated PBMCs, and LCLs.

bioRxiv preprint doi: https://doi.org/10.1101/2020.02.12.945469; this version posted February 12, 2020. The copyright holder for this preprint (which was not certified by peer review) is the author/funder, who has granted bioRxiv a license to display the preprint in perpetuity. It is made available under aCC-BY 4.0 International license.

Supporting information

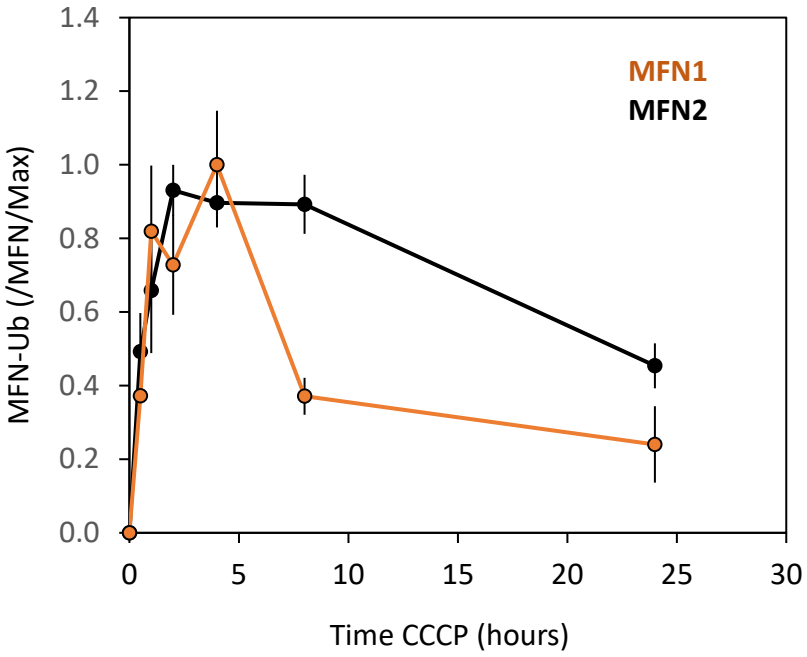

S1 Fig. Time course analysis of MFN ubiquitination in Jurkat cells. Jurkat cells were treated with 20 µM CCCP for increasing periods of time and the ubiquitination of MFN1/MFN2 was analysed by immunoblotting. The levels of ubiquitinated MFN1 and MFN2 were quantified relative to the respective non-ubiquitinated protein. Graph represents mean ± SEM; MFN1, n=2; MFN2, n=3.

bioRxiv preprint doi: https://doi.org/10.1101/2020.02.12.945469; this version posted February 12, 2020. The copyright holder for this preprint (which was not certified by peer review) is the author/funder, who has granted bioRxiv a license to display the preprint in perpetuity. It is made available under aCC-BY 4.0 International license.

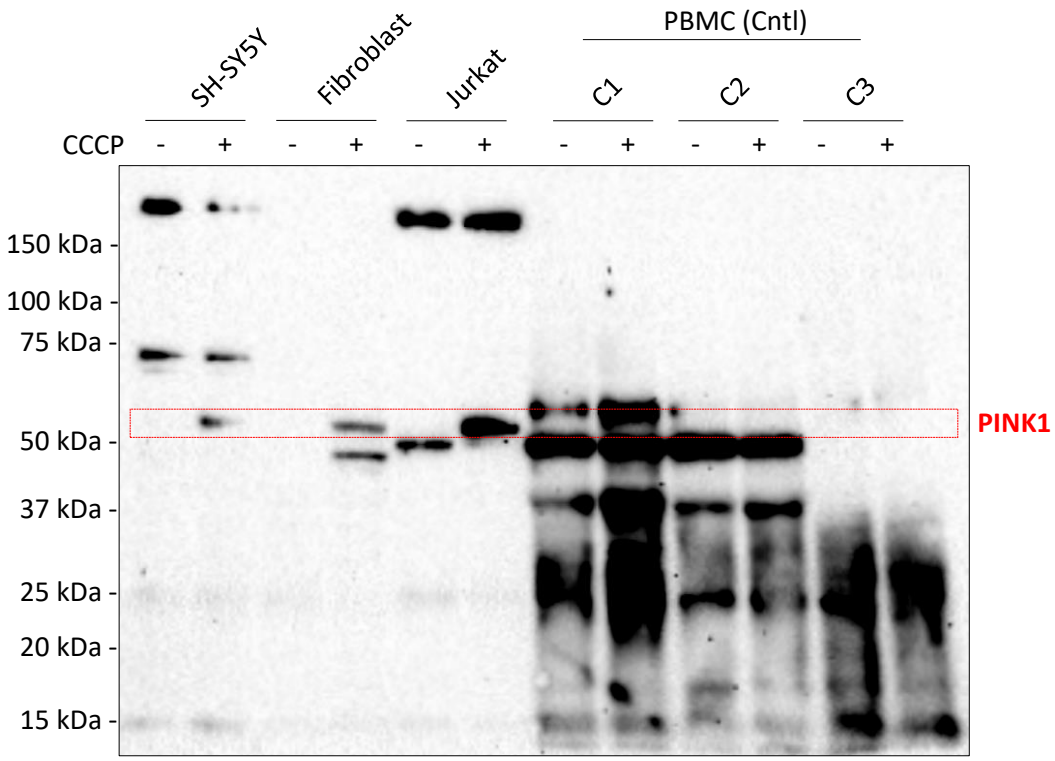

S2 Fig. Analysis of PINK1 expression in different cell types. SH-SY5Y, fibroblast, Jurkat and PBMC cultures were left untreated or treated with 20 µM CCCP for 24 hours. Samples were analysed by western blotting with the PINK1 antibody clone D8G3 (Cell Signaling Technology). PINK1 protein is indicated by the red box.

bioRxiv preprint doi: https://doi.org/10.1101/2020.02.12.945469; this version posted February 12, 2020. The copyright holder for this preprint (which was not certified by peer review) is the author/funder, who has granted bioRxiv a license to display the preprint in perpetuity. It is made available under aCC-BY 4.0 International license.

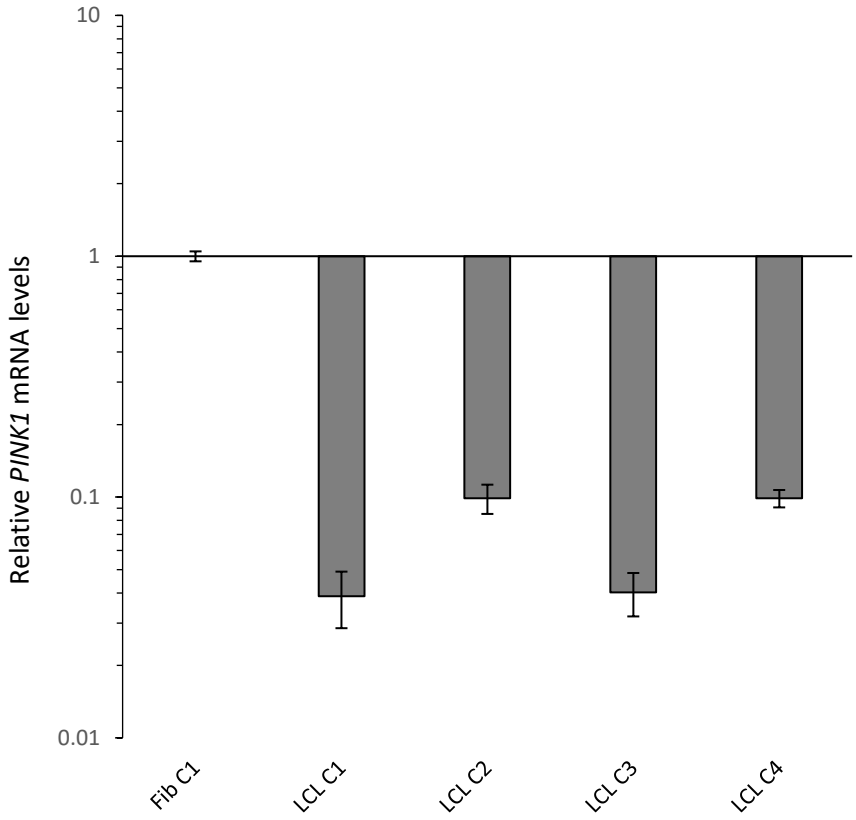

517

518 **S3 Fig. Reverse transcriptase qPCR analysis of *PINK1* in LCLs.** qPCR was performed on equal
519 amounts of cDNA from each cell sample, and C_t values were expressed relative to the fibroblast (Fib)
520 sample.

521

522

523

524

525

526

527

528

529

530

531

532

533

534

535

bioRxiv preprint doi: https://doi.org/10.1101/2020.02.12.945469; this version posted February 12, 2020. The copyright holder for this preprint (which was not certified by peer review) is the author/funder, who has granted bioRxiv a license to display the preprint in perpetuity. It is made available under aCC-BY 4.0 International license.

S4 Table. Age and sex of PBMC donors.

PBMC	Age	M/F
C1	31.2	F
C2	26.4	M
C3	25.3	M
C4	28.6	M
C5	60.1	M
C6	64.2	M
C7	66.9	M
C8	74.2	F
C9	27.7	M
C10	58.8	F
C11	31.4	F
C12	50.4	M
C13	34.1	F
C14	58.8	F
C15	72.8	M
C16	64.6	M

bioRxiv preprint doi: https://doi.org/10.1101/2020.02.12.945469; this version posted February 12, 2020. The copyright holder for this preprint (which was not certified by peer review) is the author/funder, who has granted bioRxiv a license to display the preprint in perpetuity. It is made available under aCC-BY 4.0 International license.

556 **S5 Table.** Characteristics of antibodies used in this study.

Target	Host	Cat. No. (Supplier)	Immunogen	Clone	Dilution
MFN1	Ms mAB	ab57602 (Abcam)	Human Mitofusin 1 aa 1-741.	[3C9]	1:1000
MFN2	Ms mAB	ab56889 (Abcam)	Human Mitofusin 2 aa 661-757	[6A8]	1:1000
SDHA	Ms mAB	ab14715 (Abcam)	Full length native protein	[2E3GC12FB2AE2]	1:1000
bActin	Ms mAB	ab3280 (Abcam)	Chicken Actin aa 50-70	[C4]	1:1000
Parkin	Rb mAB	702785 (Thermo Fisher Scientific)	human Parkin aa 1 465	[21H24L9]	1:100
Parkin	Ms mAB	4211 (Cell Signaling Technology)	human recombinant parkin	[Prk8]	1:500
PINK1	Rb pAB	BC100-494 (Novus Biological)	Human PINK1 protein aa 175-250		1:1000
PINK1	Rb mAB	6946 (Cell Signaling Technology)	residues surrounding aa 140 of human PINK1 protein	[D8G3]	1:1000

557